

¹State Key Laboratory of Cell Biology, Shanghai Institute of Biochemistry and Cell Biology, Center for Excellence in Molecular Cell Science, Chinese Academy of Sciences, Shanghai 200031, China;

²University of Chinese Academy of Sciences, Beijing 100049, China;

³Department of Pulmonary Medicine, ZhongShan Hospital, Fudan University, Shanghai 200032, China;

⁴Division of Hematology and Medical Oncology, Laura and Isaac Perlmutter Cancer Center, New York University Langone Medical Center, New York, NY 10016, USA;

⁵College of Life Sciences, Qufu Normal University, Qufu 273165, China;

⁶Shanghai University of Medicine and Health Sciences, Shanghai Sixth People's Hospital East Campus, Shanghai 201306, China;

⁷Department of General Surgery, Shanghai Jiao Tong University Affiliated Sixth People's Hospital, Shanghai 200233, China;

⁸Department of Thoracic Surgery, Fudan University Shanghai Cancer Center, Shanghai 200032, China;

⁹School of Life Science and Technology, Shanghai Tech University, Shanghai 200120, China and

¹⁰School of Life Science, Hangzhou Institute for Advanced Study, University of Chinese Academy of Sciences, Hangzhou 310024, China

***Corresponding**

authors. E-mails: hbji@sibcb.ac.cn; liang.hu@sibcb.ac.cn; sun.yihua76@hotmail.com

[†]Equally contributed to this work.

Received 7 September 2020; **Revised** 23 December 2020;

Accepted 18 January 2021

MOLECULAR BIOLOGY & GENETICS

Targeting HSPA1A in ARID2-deficient lung adenocarcinoma

Xue Wang^{1,†}, Yuetong Wang^{1,2,†}, Zhaoyuan Fang^{1,†}, Hua Wang¹, Jian Zhang^{1,2}, Longfu Zhang³, Hsinyi Huang¹, Zhonglin Jiang^{1,2}, Yujuan Jin¹, Xiangkun Han¹, Shenda Hou¹, Bin Zhou¹, Feilong Meng¹, Luonan Chen¹, Kwok-Kin Wong⁴, Jinfeng Liu⁵, Zhiqi Zhang^{6,7}, Xin Zhang³, Haiquan Chen⁸, Yihua Sun^{8,*}, Liang Hu^{1,*} and Hongbin Ji^{1,9,10,*}

ABSTRACT

Somatic mutations of the chromatin remodeling gene ARID2 are observed in ~7% of human lung adenocarcinomas (LUADs). However, the role of ARID2 in the pathogenesis of LUADs remains largely unknown. Here we find that ARID2 expression is decreased during the malignant progression of both human and mice LUADs. Using two *Kras*^{G12D}-based genetically engineered murine models, we demonstrate that ARID2 knockout significantly promotes lung cancer malignant progression and shortens overall survival. Consistently, ARID2 knockdown significantly promotes cell proliferation in human and mice lung cancer cells. Through integrative analyses of ChIP-Seq and RNA-Seq data, we find that *Hspa1a* is up-regulated by *Arid2* loss. Knockdown of *Hspa1a* specifically inhibits malignant progression of *Arid2*-deficient but not *Arid2*-wt lung cancers in both cell lines as well as animal models. Treatment with an HSPA1A inhibitor could significantly inhibit the malignant progression of lung cancer with ARID2 deficiency. Together, our findings establish ARID2 as an important tumor suppressor in LUADs with novel mechanistic insights, and further identify HSPA1A as a potential therapeutic target in ARID2-deficient LUADs.

Keywords: lung adenocarcinoma, tumor suppressor, ARID2, HSPA1A

INTRODUCTION

Chromatin remodeling is known to play important roles in multiple physiological as well as pathological settings [1,2]. Conserved from yeast to human, the SWI/SNF (switch/sucrose nonfermenting) complex, as the essential component of chromatin remodelers, is involved in cell differentiation, proliferation and the DNA repair process [3,4]. The SWI/SNF complex, consisting of ~15 subunits including lineage-specific variants, can slide the nucleosome along DNA in an adenosine triphosphate (ATP)-dependent manner and control lineage-specific gene expression via combinatorial assembling [2]. Loss of function of the SWI/SNF complex is potentially associated with disease malignant transformation [1]. Individual components of SWI/SNF complex are frequently mutated in cancer

and the collective mutation rates for this complex vary among epithelial cancers, e.g. 75% in ovarian clear cell carcinoma [5], 57% in clear cell renal cell carcinoma [6], 40% in hepatocellular carcinoma [7], 34% in melanoma [8] and 35.12% in lung cancer [9].

BAF (Brg/Brahma-associated factors) and PBAF (Polybromo-associated BAF) are two variant forms of the SWI/SNF chromatin-remodeling complex. These two forms share many subunits but have also subtype specific subunits: BAF250 and hBRM are only found in BAF, whereas BAF180 and BAF200 are only found in PBAF [10]. BAF200, which is encoded by ARID2, is required for the function and selectivity of PBAF. Knockdown of ARID2 may affect the protein levels of other PBAF subunits as well as the function of PBAF in development and

differentiation [11,12]. ARID2 is currently considered as a tumor suppressor gene since its nonsense mutations found in ~10% melanoma samples are predicted to be loss-of-function mutations and lack the capability for DNA binding [8]. The inactivating mutation rate of ARID2 is ~18.2% of HCV-associated hepatocellular carcinomas in the US and Europe [7,13]. In addition, ARID2 is also listed as one of the most frequently mutated genes after TP53, KRAS, EGFR, CDKN2A and STK11 (or LKB1) with an inactivating mutation rate ~7.3% in lung adenocarcinomas (LUADs), the major subtype of lung cancer [14,15]. However, the contribution of ARID2 to the malignant progression of LUADs remains largely uncharacterized.

In this study, we found that ARID2 expression was decreased during the malignant progression of LUADs. Using autochthonous mouse models of lung cancer [16,17], we demonstrated a tumor suppressive role of ARID2 in LUADs. Moreover, we identified HSPA1A as a potential target for ARID2-deficient LUADs.

RESULTS

ARID2 expression is decreased during the malignant progression of LUADs

Through immunostaining analyses of 63 human LUAD samples (Fig. 1A), we found that ARID2 expression was significantly decreased with disease malignant progression (Fig. 1B). Moreover, we found that those patients with low ARID2 expression were associated with poor survival (Fig. 1C) (<http://www.kmplot.com/lung>) [18].

To evaluate the expression levels of ARID2 during the development and progression of LUADs *in vivo*, we employed a well-established autochthonous LUAD mouse model driven by *Kras*^{G12D} mutant [16]. Lox-Stop-Lox *Kras*^{G12D/+} (K) mice were treated with Ade-Cre through nasal inhalation to induce lung tumors as described previously [19]. After 24 weeks of Ade-Cre administration, the lungs of K mice exhibited multifocal and heterogeneous lesions, including atypical adenomatous hyperplasia (AAH, grade I), adenoma (grade II) and adenocarcinoma (grade III, Fig. 1D). We found that ARID2 expression was progressively decreased from AAH, adenoma, to adenocarcinoma in this model (Fig. 1E and F). Meanwhile, Ki-67 staining was gradually increased with disease malignant progression, consistent with an increased proliferation index from AAH to adenocarcinoma (Fig. 1E and F). These results indicate that ARID2 might act as a candidate tumor suppressor in LUADs.

ARID2 deletion facilitates malignant progression of autochthonous lung cancer

Next, we determined the effects of ARID2 deletion *in vivo*. We found that *Arid2*^{fl/fl} mice did not develop detectable lung tumors even after 70 weeks of Ade-Cre administration (Fig. S1A and B), indicating that ARID2 deletion alone is insufficient to drive lung tumor formation.

To evaluate the role of ARID2 in the pathogenesis of autochthonous mouse models of lung cancer, we first crossed the *Arid2*^{fl/fl} mice to K mice to generate the *Kras*^{G12D/+}*Arid2*^{fl/fl} (KA) mice. We treated K or KA mice with Ade-Cre through nasal inhalation [19] and used the *Kras*^{G12D/+}*Lkb1*^{fl/fl} (KL) mice as a positive control (Fig. 2A), which is well-known for highly malignant tumors [17]. We confirmed *Lkb1* and *Arid2* deletion by polymerase chain reaction (PCR) genotyping (Fig. S1C). Notably, KA mice had much shorter survival than K mice, with a median time comparable to KL mice (Fig. 2B). Histopathological analyses confirmed that ARID2 deletion greatly promoted the malignant progression of lung cancer in K mice (Fig. 2C). Both tumor number and tumor burden were significantly increased in KA mice (Fig. 2D and E). Consistently, increased Ki-67 staining was observed in KA tumors (Fig. 2F and G).

We further crossed the *Arid2*^{fl/fl} mice to KL mice and generated the *Kras*^{G12D/+}*Lkb1*^{fl/fl}*Arid2*^{fl/fl} (KLA) cohort. The KLA or KL mice were then treated with Ade-Cre via nasal inhalation (Fig. 2H) and the efficiency of *Lkb1* and *Arid2* deletion was confirmed by PCR genotyping (Fig. S1C). The KLA mice had a much shorter survival than KL mice (Fig. 2I). After six weeks of Ade-Cre treatment, larger tumors were frequently observed in KLA mice compared to KL mice (Fig. 2J). Moreover, an increased number of grade II and III tumors and a decreased number of grade I tumors were observed in KLA mice (Fig. 2K). Consistently, increased tumor burden and Ki-67 staining were observed in KLA mice (Fig. 2L–N). All the KLA mice (5/5) developed metastases into lymph node, liver and chest wall as early as seven weeks post-Ade-Cre treatment (Fig. S2A). In contrast, there was no detectable metastasis in KL mice (0/5) at the same time point. Primary tumors and metastatic lesions kept proliferative and positive for the LUAD biomarker TTF1 (Fig. S2B). We further established a KLA tumor-derived primary cell line (hereafter referred to as KLA cells) (Fig. S2C) and found that ectopic expression of ARID2 significantly inhibited the migratory capability of KLA cells (Fig. S2D and E). These data strongly suggest a tumor-suppressive role for ARID2 in lung cancer malignant progression.

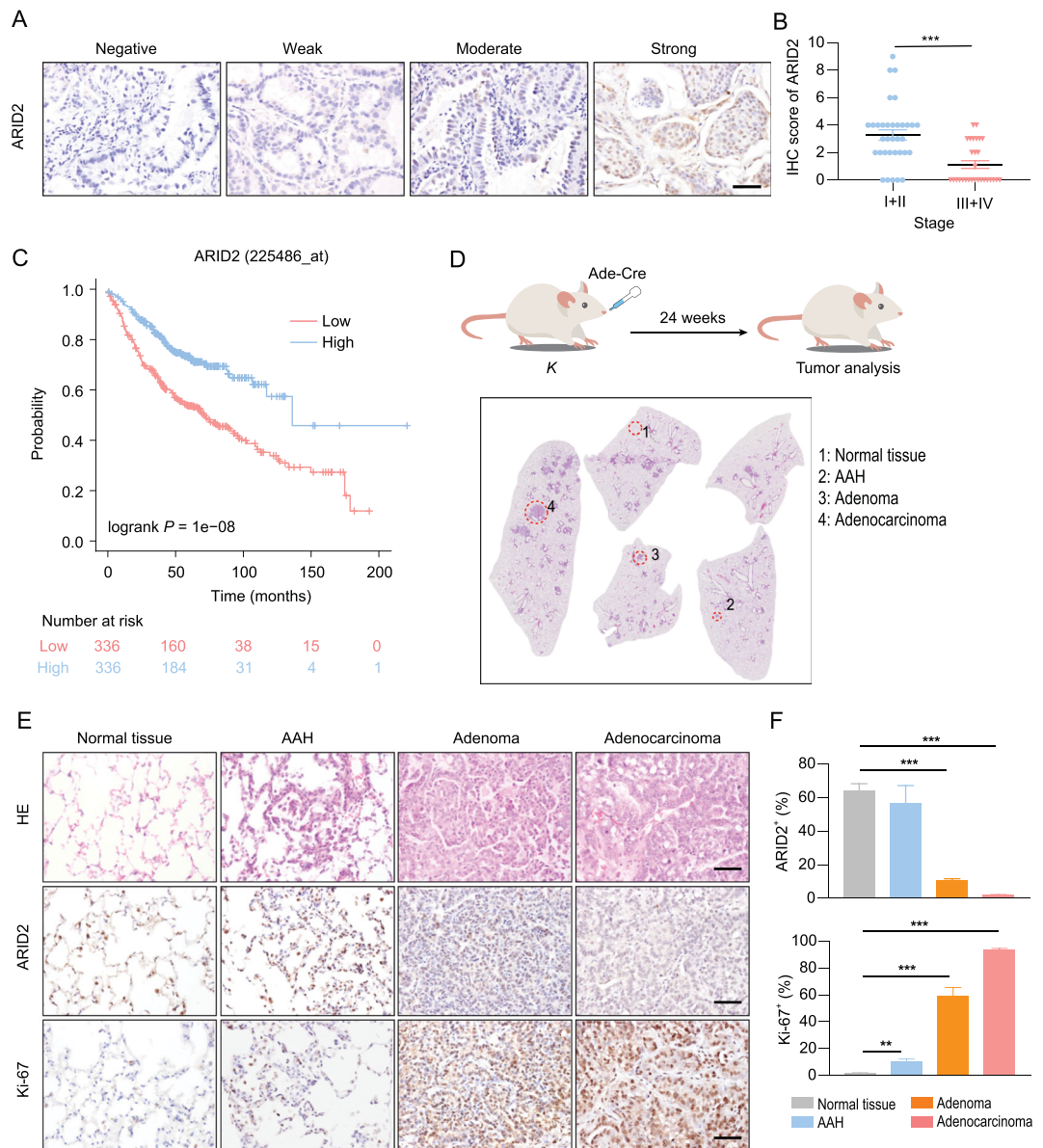


Figure 1. ARID2 expression is decreased during LUAD malignant progression. (A) ARID2 immunostaining in human LUAD. Representative photos for different expression levels. Scale bar: 50 μm . (B) Statistical analysis of ARID2 expression in 63 human LUADs with different stages. Stage I (n = 17), Stage II (n = 17), Stage III (n = 25) and Stage IV (n = 4). (C) Kaplan-Meier survival curve. (D) Schematic illustration of *Kras*-driven lung cancer mouse model and histopathological phenotype was shown. *K* mice at 6–8 weeks old were treated with 2×10^6 p.f.u. Ade-Cre via nasal inhalation and analyzed at 24 weeks after Ade-Cre administration. (E and F) Representative HE and immunostaining (E) and quantification (F) of ARID2 and Ki-67 expression in *K* mice with different histopathological phenotypes. Scale bars: 50 μm . ** $P < 0.01$, *** $P < 0.001$.

Knockdown of ARID2 accelerates cell proliferation in human and mice lung cancer cells

To evaluate the role of ARID2 *in vitro*, we depleted ARID2 in human LUAD cell lines H1944 and H1373 and found that ARID2 knockdown significantly promoted cell growth, which could be rescued by ARID2 re-expression (Fig. 3A, and Fig. S3A

and B). Next, we sought to confirm the function of ARID2 in primary cells derived from mouse tumors. Since it is difficult to establish primary cell lines from *K* tumors, we employed a *KL* tumor-derived primary cell line (hereafter refer to as *KL* cells) to perform subsequent *in vitro* and *in vivo* studies. Consistently, ARID2 knockdown accelerated *KL* cell proliferation, which could be reversed by ARID2 re-expression (Fig. 3A, and Fig. S3A and B).

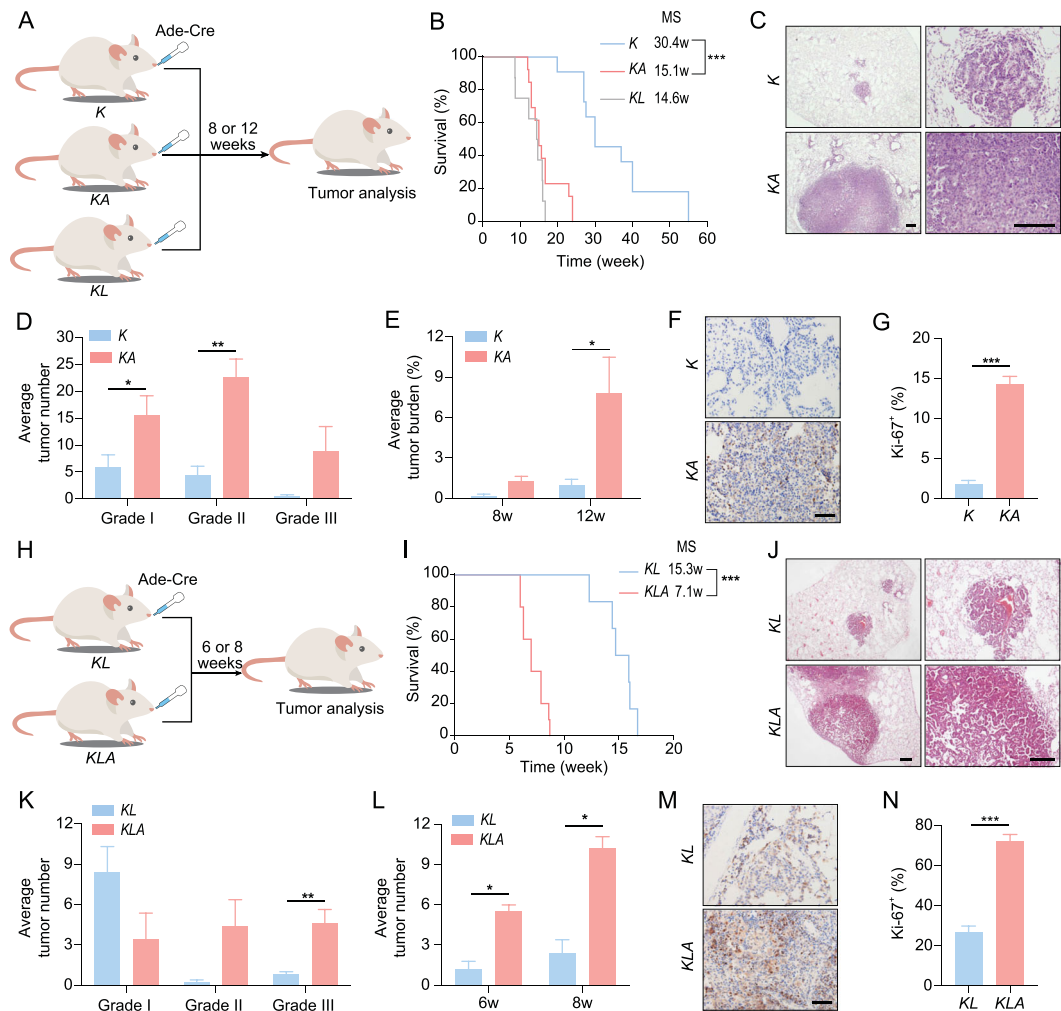


Figure 2. ARID2 depletion facilitates murine lung cancer malignant progression. (A) Schematic illustration of *K*, *KA* and *KL* mouse models. (B) Kaplan-Meier survival curves. MS, median survival time. (C) Representative histology of lung tumors from *K* and *KA* mice at 12 weeks post-Ade-cre treatment. Scale bar: 200 μm . (D and E) Quantification of tumor number (D) and burden (E); $n = 5$. (F) Representative Ki-67 immunostaining. Scale bars: 50 μm . (G) Quantification of Ki-67 immunostaining. (H) Schematic illustration of *KL* and *KLA* mouse models. (I) Kaplan-Meier survival curves. (J) Representative histology of lung tumors from *KL* and *KLA* mice at six weeks post-Ade-cre treatment. Scale bars: 200 μm . (K and L) Quantification of tumor number (K) and burden (L); $n = 5$. (M) Representative Ki-67 immunostaining. Scale bar: 50 μm . (N) Quantification of Ki-67 immunostaining. * $P < 0.05$, ** $P < 0.01$, *** $P < 0.001$.

Moreover, ARID2 knockdown significantly promoted *KL* tumor growth (Fig. 3B and C). Immunohistochemical analysis revealed that ARID2-knockdown tumors had increased Ki-67 positive staining compared with control counterparts (Fig. 3D and E). No substantial difference in the positive staining of cleaved-caspase-3 (CC-3) was observed between the ARID2-knockdown and control groups (Fig. 3D and E), indicating that ARID2 mainly suppresses proliferation of lung cancer cells. These data further solidify the role of ARID2 as a lung tumor suppressor.

ARID2 knockout transcriptionally up-regulates *HSPA1A* expression potentially through a de-repression mechanism

ARID2 is a core component of the SWI/SNF chromatin-remodeling complex and regulates downstream gene transcription [11,20]. The ARID2-containing PBAF chromatin regulatory complex activates or represses gene transcription depending on different binding sites and/or co-factors [21,22]. To examine the possible mechanism

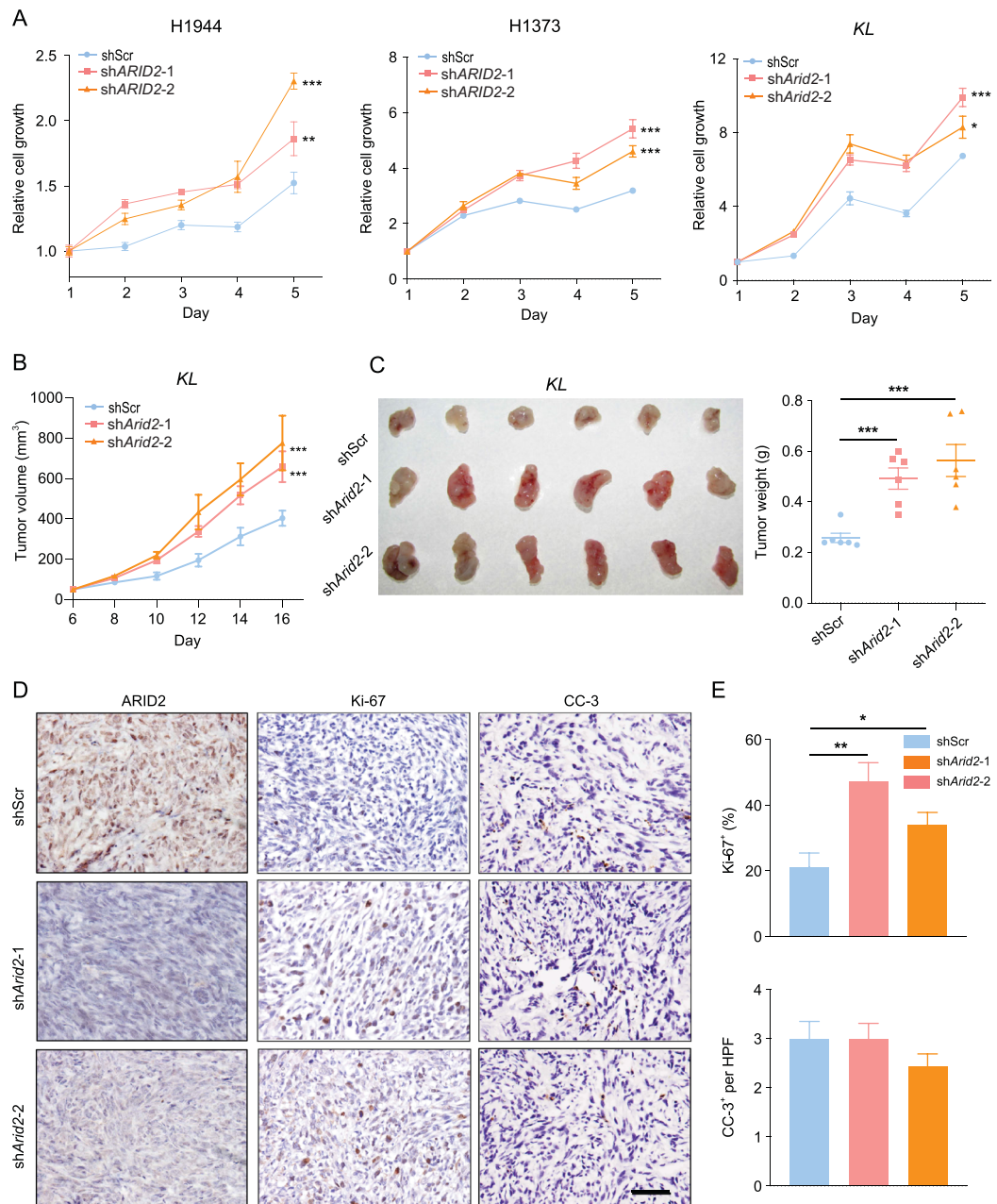


Figure 3. ARID2 knockdown accelerates human and mice lung cancer cell proliferation. (A) Relative growth curve of human LUAD cell lines H1944, H1373 and mouse *KL* cells with or without ARID2 knockdown. (B) Tumor growth of *KL* allografts with or without ARID2 knockdown; $n = 6$. (C) Photos and tumor weight of *KL* tumors with or without ARID2 knockdown. (D) Representative immunostaining of ARID2, Ki-67 and CC-3 in *KL* tumors with or without ARID2 knockdown. Scale bar: $50 \mu\text{m}$. (E) Quantification of Ki-67 and CC-3 immunostaining. * $P < 0.05$, ** $P < 0.01$, *** $P < 0.001$.

by which ARID2 exerts its tumor suppressive function in LUADs, we performed RNA-Seq analysis to compare differentially expressed genes between *KA* versus *K* tumors and *KLA* versus *KL* tumors, and identified a list of genes consistently up-regulated in ARID2-deficient tumors (Table S1).

To narrow down the list, we use *KL* cells for ARID2 ChIP-seq to identify genes directly regu-

lated by ARID2 (Fig. 4A). Through integrative analyses of the consistently up-regulated genes, ARID2 ChIP-seq data and survival-related genes from the cancer genome atlas (TCGA)-LUAD dataset, we found three candidate genes including *Hspa1a*, *Pkm* and *Tsku* (Fig. 4A). *Hspa1a* belongs to the heat shock protein 70 (HSP70) family and is implicated in cancer development and drug sensitivity

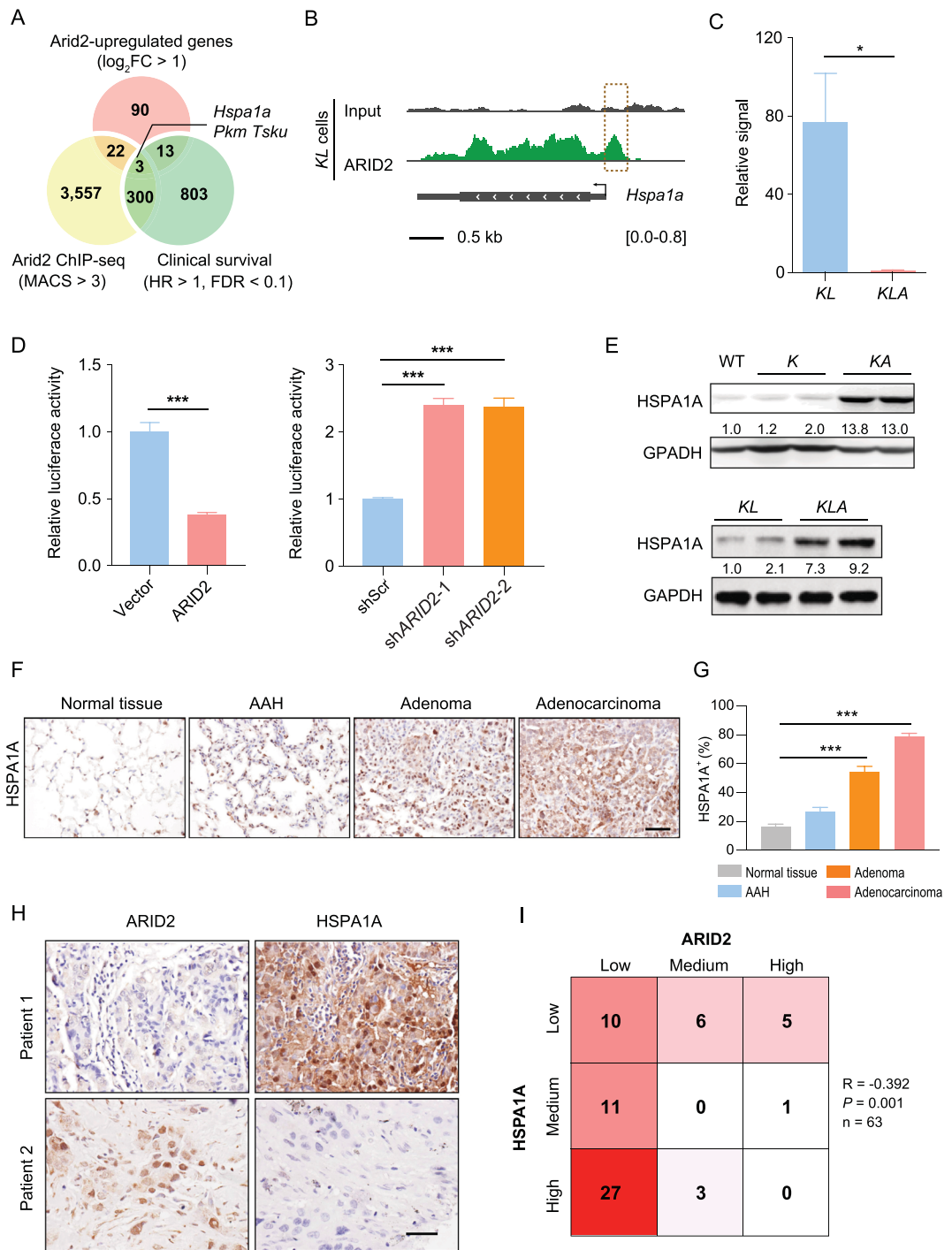


Figure 4. ARID2 loss transcriptionally up-regulates *HSPA1A* expression potentially through a de-repression mechanism. (A) Venn diagram of up-regulated genes in ARID2-loss tumors, ARID2 binding genes by ARID2 ChIP-seq and clinical survival-related genes from the TCGA-LUAD dataset. (B) ARID2 ChIP-seq of ARID2 binding signals along the promoter regions of *Hspa1a* genes in KL cells. Dashed box marks ARID2 binding peaks. (C) ChIP-qPCR assay confirmed the binding of ARID2 to the promoter region of *Hspa1a* gene in KL cells. Y axis shows the signal of *Hspa1a* promoter region relative to irrelevant primer. (D) Luciferase reporter assay in 293T cells with ARID2 overexpression or knockdown. (E) Western blot detection of HSPA1A expression in tumors from different mouse models. (F and G) Representative immunostaining (F) and quantification (G) of HSPA1A expression in K mice with different histopathological phenotypes at 24 weeks post-Ade-Cre treatment. Scale bar: 50 μm . (H) Representative immunostaining of ARID2 and HSPA1A in two human LUAD samples. Scale bar: 50 μm . (I) Correlation analysis of ARID2 and HSPA1A expression in human LUAD samples. * $P < 0.05$, *** $P < 0.001$.

[23]. ARID2 ChIP-seq data revealed the distribution of ARID2 binding signals along the *Hspa1a* promoter region (Fig. 4B). Public human cell line ChIP-seq dataset also supported *HSPA1A* as a potential target of ARID2 (Fig. S4A). ChIP-qPCR in *KL* and *KLA* cells showed that ARID2 can bind to the promoter region of *Hspa1a* gene, which could be abolished upon ARID2 loss (Fig. 4C). We further performed luciferase reporter gene assay and found that ectopic ARID2 expression suppressed *Hspa1a* promoter activity, and vice versa (Fig. 4D and Fig. S4B). These data suggest that ARID2 loss promotes *HSPA1A* expression potentially through a transcriptional de-repression mechanism. Consistently, lung tumors with *Arid2* knockout (*KA* and *KLA*) showed higher levels of *HSPA1A* protein (Fig. 4E). Moreover, protein levels of *HSPA1A* progressively increased from AAH, adenoma, to adenocarcinoma in *K* mice after 24 weeks of Ade-Cre treatment (Fig. 4F and G). We further found that protein levels of ARID2 were inversely correlated with *HSPA1A* in 63 LUAD specimens ($R = -0.392$; $P = 0.001$) (Fig. 4H and I). We also observed a significant association between high *HSPA1A* expression and ARID2 mutation in 257 LUAD samples without *HSPA1A* genetic alterations from the TCGA database (Fig. S4C).

HSPA1A knockdown preferentially suppresses the malignant progression of ARID2-deficient LUADs

To determine the role of *HSPA1A* depletion in the malignant progression of ARID2-deficient LUADs *in vivo*, we treated *K* or *KA* mice with lentivirus-mediated shRNA targeting *Hspa1a* through nasal inhalation (Fig. 5A). *Hspa1a* knockdown dramatically decreased tumor burden and number in *KA* mice without significant impact upon *K* mice (Fig. 5B–E and Fig. S5). Consistently, decreased Ki-67 staining and increased CC-3 staining were observed in *HSPA1A*-knockdown *KA* tumors (Fig. 5F–I). In contrast, no significant effect upon proliferation or apoptosis was observed in *K* tumors following *HSPA1A* knockdown (Fig. 5F–I). These data suggest that *HSPA1A* knockdown exerts superior antitumor effects in ARID2-deficient LUADs in mice.

Genetic or pharmacological inhibition of HSPA1A specifically dampens ARID2-deficient lung tumor growth

We further found that *HSPA1A* knockdown significantly inhibited the *KLA* cell proliferation,

which could be reversed by *HSPA1A* re-expression (Fig. 6A, and Fig. S6A and B). In contrast, knockdown of *HSPA1A* in *KL* cells did not apparently affect cell growth (Fig. 6A and Fig. S6A). We also found that ectopic *HSPA1A* expression promoted *KL* cell growth (Fig. S6C and D). Since *HSPA1A* has been implicated in cell apoptosis [24], we performed Annexin V/PI staining and found that *HSPA1A* knockdown specifically increased cell apoptosis in *KLA* cells but not in *KL* cells (Fig. 6B and Fig. S6E–G). Knockdown of *HSPA1A* also greatly suppressed the migratory capability of *KLA* cells (Fig. S6H and I). More importantly, *HSPA1A* knockdown significantly inhibited malignant progression of *KLA* allograft tumors (Fig. 6C, and Fig. S6J and K). Decreased Ki-67 staining and increased CC-3 staining were observed in *HSPA1A*-knockdown groups (Fig. 6D and E). These findings suggest that ARID2-deficient cancer cells preferentially rely on *HSPA1A* for cell proliferation, survival and migration, which provides the vulnerability for therapeutic targeting.

KNK437 was reported as a specific *HSPA1A* inhibitor which is well tolerated in immunocompromised mice [25]. We found that KNK437 treatment decreased *HSPA1A* protein levels *in vitro* and *in vivo* (Fig. 6F and Fig. S9A). Moreover, the IC₅₀ value of KNK437 was significantly lower in *KLA* cells (0.05 mM) than *KL* cells (1 mM) (Fig. 6G). Consistent with the effects of *HSPA1A* knockdown, KNK437 treatment triggered overt cell apoptosis in *KLA* cells (Fig. 6H and Fig. S9B). These observations were further confirmed using another *HSPA1A*-specific inhibitor apoptozole [26] (Fig. 6I–K, and Fig. S9C).

Through analysis of the LUAD-TCGA database, we noticed that ARID2 mutations were almost evenly distributed along its open reading frame (ORF) region (Fig. S7A), indicative of the lack of hotspot mutations. COSMIC data showed that the human LUAD cell line H23 harbored an ARID2 mutation (452M>V). The IC₅₀ of KNK437 in H23 cells was ~0.14 mM (Fig. S7B), which was much lower than *KL* cells and comparable to *KLA* cells (Fig. 6G). The ARID2 M452V mutation was a loss-of-function mutation, as ectopic expression of wild-type ARID2, but not ARID2^{M452V} mutant, suppressed the *HSPA1A* expression and inhibited cell proliferation (Fig. S8A–C). Furthermore, either KNK437 treatment or *HSPA1A* knockdown preferentially suppressed the growth of *KLA* cells expressing ARID2^{M452V} mutant (Fig. S8D and E). Additionally, human liver cancer cell line SNU-398 (ARID2 mutant) was more sensitive to KNK437 than HepG2 (ARID2 wild-type) (Fig. S7B). These observations indicate that cancer

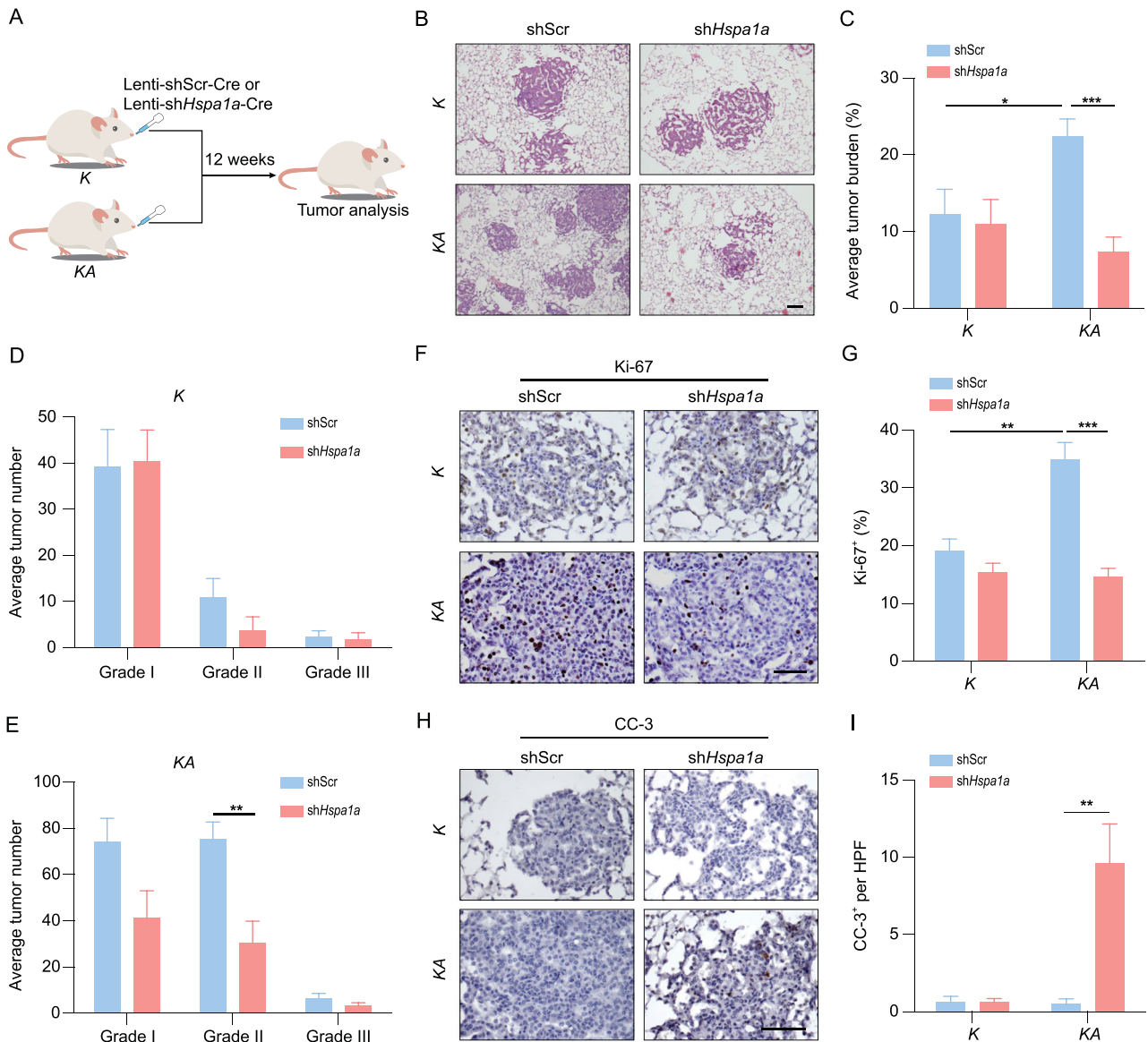


Figure 5. HSPA1A knockdown preferentially suppresses the malignant progression of ARID2-deficient LUADs. (A) Schematic illustration of HSPA1A knockdown in *K* and *KA* mouse models. (B) Representative histology of lung tumors from *K* and *KA* mice with or without HSPA1A knockdown at 12 weeks post-Lenti-cre treatment. Scale bar: 100 μ m. (C–E) Quantification of tumor burden (C) and number (D and E) of *K* and *KA* mice with or without HSPA1A knockdown at 12 weeks post-Lenti-Cre treatment; $n = 5$. (F and G) Representative immunostaining (F) and quantification (G) of Ki-67 expression in tumors from *K* and *KA* mice with or without HSPA1A knockdown. Scale bar: 50 μ m. (H and I) Representative immunostaining (H) and quantification (I) of CC-3 expression in tumors from *K* and *KA* mice with or without HSPA1A knockdown. Scale bar: 100 μ m. * $P < 0.05$, ** $P < 0.01$, *** $P < 0.001$.

cell lines harboring ARID2 mutations might be vulnerable to HSPA1A inhibition.

Importantly, KNK437 treatment greatly inhibited the growth of *KLA* allograft tumors without significant impact upon *KL* counterparts (Fig. 6L and M and Fig. S9D). Consistently, decreased Ki-67 staining and increased CC-3 staining were observed in KNK437-treated *KLA* tumors (Fig. 6N and O). These findings suggest that pharmacological inhi-

bition of HSPA1A selectively suppresses ARID2-deficient lung tumor growth.

DISCUSSION

Here we demonstrate that ARID2 acts as an important tumor suppressor gene in LUADs and reveal that ARID2 depletion induces HSPA1A expression potentially through a transcriptional de-repression

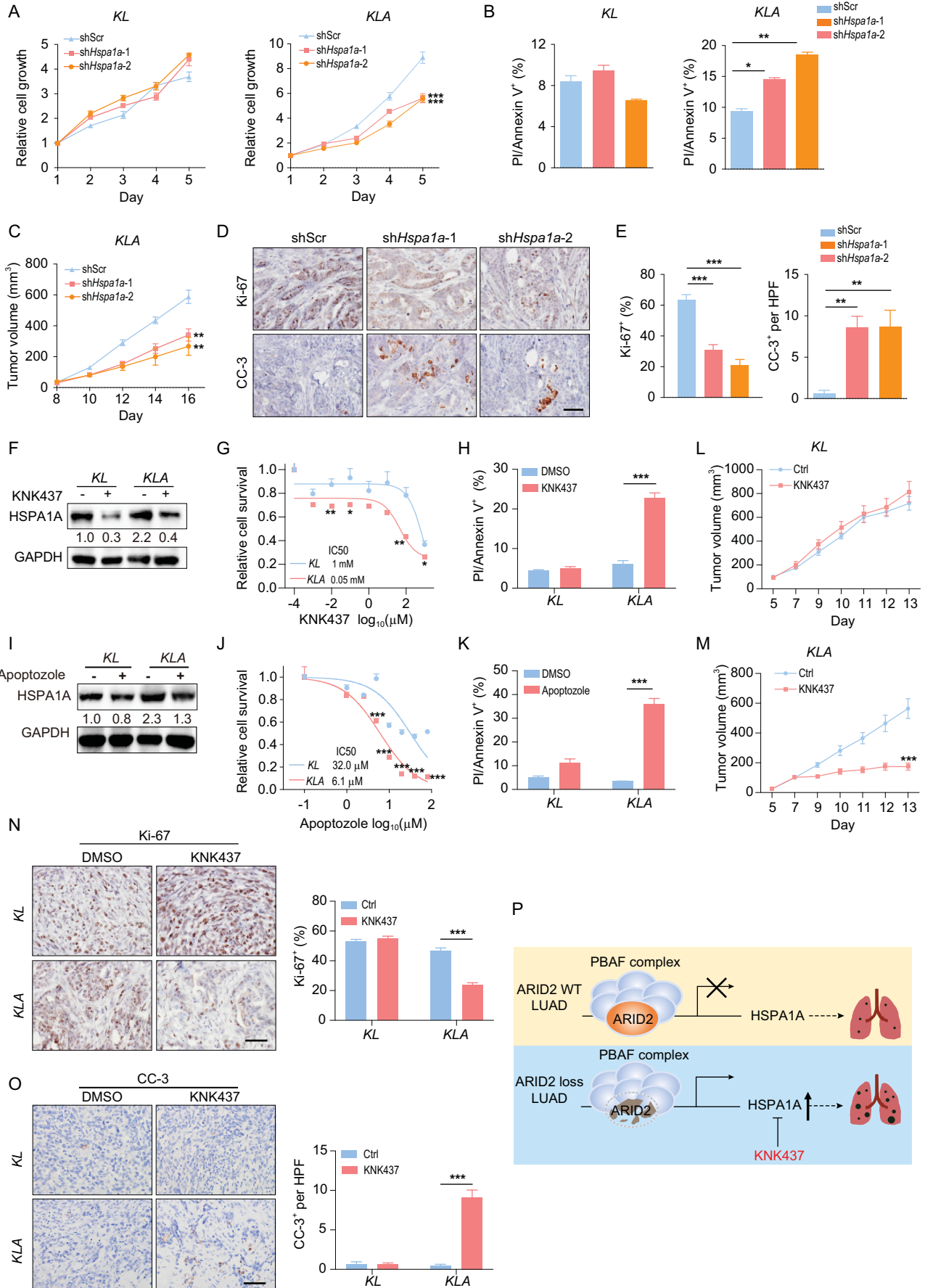


Figure 6. Genetic or pharmacological inhibition of HSPA1A specifically dampens ARID2-deficient lung tumor growth. (A) Relative growth curve of *KL* and *KLA* cells with or without HSPA1A knockdown. (B) Quantification of PI/Annexin V staining in *KL* and *KLA* cells with or without HSPA1A knockdown. (C) Tumor growth of *KLA* allografts with or without HSPA1A knockdown; $n = 5$. (D and E) Representative immunostaining (D) and quantification (E) of Ki-67 and CC-3 expression in *KLA* tumors with or without HSPA1A knockdown. Scale bar: 50 μm . (F) Western blot detection of HSPA1A expression in *KL* and *KLA* cells with or without KNK437 treatment. (G) Dose response curves of KNK437 treatment in *KL* and *KLA* cells. (H) Quantification of the PI/Annexin V staining in *KL* and *KLA* cells with or without KNK437 treatment. (I) Western blot detection of HSPA1A expression in *KL* and *KLA* cells with or without Apoptozole treatment. (J) Dose response curves of Apoptozole treatment in *KL* and *KLA* cells. (K) Quantification of the PI/Annexin V staining in *KL* and *KLA* cells with or without Apoptozole treatment. (L and M) Tumor growth of *KL* (L) and *KLA* (M) allografts with or without KNK437 treatment. (N and O) Representative immunostaining and quantification of Ki-67 (N) and CC-3 (O) expression in *KL* and *KLA* tumors with or without KNK437 treatment. Scale bar: 50 μm . (P) Working model. ARID2 loss accelerates the malignant progression of LUAD potentially through HSPA1A. * $P < 0.05$, ** $P < 0.01$, *** $P < 0.001$.

mechanism. Importantly, genetic and pharmacological inhibition of HSPA1A exhibit impressive therapeutic effects in ARID2-deficient tumors, suggesting that targeting HSPA1A may be an effective strategy in ARID2-mutant LUADs (Fig. 6P).

High frequency of ARID2 mutation has been documented in different types of human cancers including lung cancer [15,27,28]. Loss-of-function mutations of ARID2 have been reported to be observed in $\sim 7.3\%$ of LUADs [15]. However, the role of ARID2 in LUAD development remains largely unknown. Using clinical specimens and autochthonous mouse models of lung cancer, we provide strong evidence to illustrate a tumor suppressive role of ARID2 in LUADs.

In an attempt to search for the molecular events involved in mediating the effect of ARID2 depletion, we find that HSPA1A is one of the significantly up-regulated genes in ARID2-deficient lung tumors. Through RNA-seq, ChIP-seq, ChIP-qPCR and luciferase reporter assay, we demonstrate that ARID2 depletion transcriptionally up-regulates *Hspa1a* expression potentially through a transcriptional de-repression mechanism. The inverse correlation between ARID2 and HSPA1A expression is also observed in human LUADs. Importantly, genetic or pharmacological inhibition of HSPA1A preferentially inhibits malignant progression of ARID2-deficient LUADs in autochthonous genetically engineered murine models and allograft models. These findings not only support an essential role for HSPA1A in mediating the effects of ARID2 loss, but also identify HSPA1A as a potential vulnerable target in ARID2-deficient LUADs.

HSP70 proteins play essential roles in regulation of correct protein folding and maintenance of protein homeostasis [29]. These proteins enhance cell survival following a multitude of stresses, including elevated temperature, hypoxia, oxidative stress, altered pH, heavy metals and others [30]. The pro-survival role of HSP70 proteins is related to their ability to buffer the toxicity of denatured and misfolded proteins that accumulate during stress [24]. The HSP70 family consists of at least eight members with molecular chaperones of ~ 70 kDa in size

[29]. High expression of HSP70 has been correlated with poor prognosis in cancers of the liver [31], prostate [32], colon [33] and lung [34]. Multiple inhibitors have been designed to target the enzymatic activity of HSP70 and/or its interaction with important co-chaperones [35], and some of them have been evaluated as anticancer agents in pre-clinical or clinical trials [36–38]. Although we cannot rule out the potential involvement of other genes in ARID2 loss-mediated LUAD progression, our findings of the superior efficacy of HSP70 inhibitors in ARID2-deficient tumors clearly support the functional importance of HSPA1A in this setting and provide a potential new therapeutic strategy for clinical management of lung cancer with this subtype.

METHODS

Mice cohorts and treatment

Mice were housed in a specific pathogen-free environment at the Shanghai Institute of Biochemistry and Cell Biology and treated in accordance with protocols conforming to the ARRIVE guidelines and approved by the Institutional Animal Care and Use Committee of the Shanghai Institutes for Biological Sciences, Chinese Academy of Sciences (approval number: SIBCB-S215-2101-008). *Kras*^{G12D/+} and *Lkb1*^{fl/fl} mice were originally generously provided by Dr. T. Jacks and Dr. R. Depinho, respectively. The *Arid2*^{fl/fl} transgenic mice were previously described [39]. *K*, *KA*, *KL* and *KLA* mice at 6–8 weeks old were treated with 2×10^6 p.f.u. Ade-Cre via nasal inhalation and analyzed at different time points.

Statistical analysis

The significance of differences was determined using the one-way ANOVA or Student's t-test (two-sided). $P < 0.05$ is considered to be statistically significant. The Kendall's tau correlation analysis was used to analyze the correlation between ARID2 and HSPA1A expression in human LUAD samples. Data were represented as mean \pm standard error of the mean unless otherwise indicated. All statistical

analyses were carried out using GraphPad Prism 5 software. For more methods, see Supplementary Data.

SUPPLEMENTARY DATA

Supplementary data are available at [NSR](#) online.

FUNDING

This work was supported by the National Basic Research Program of China (2017YFA0505501 to H.J.), the National Natural Science Foundation of China (grants 81902326 to X.W., 82030083 to H.J., 81872312 to H.J., 82011540007 to H.J., 31621003 to H.J., 91731314 to H.J., 81871875 to L.H., 81402371 to Y.J., 81802279 to H.H., 81602459 to Z.F.), the Strategic Priority Research Program of the Chinese Academy of Sciences (XDB19020201 to H.J.), the Basic Frontier Scientific Research Program of Chinese Academy of Sciences (ZDBS-LY-SM006 to H.J.), the International Cooperation Project of Chinese Academy of Sciences (153D31KYSB20190035 to H.J.), the National Basic Research Program of China (2020YFA0803300 to H.J.), and the Youth Innovation Promotion Association CAS (Y919S31371 to X.W.).

AUTHOR CONTRIBUTIONS

H.J., Y.W., L.H. and X.W. conceived the project. H.J., L.H. and Y.W. wrote the manuscript. X.W. and Y.W. carried out most of the experiments and analyzed the data. Z.F. performed bioinformatics analyses. H.W., J.Z., H.H., Y.J., X.H., S.H., K-K.W., J.L., Z.Z., L.Z., X.Z., H.C. and F.M. provided technical support and/or materials support as well as helpful comments. Z.J. and L.C. helped with bioinformatics analyses. B.Z. provided the *Arid2^{fl/fl}* mice. Y.S. provided clinical samples and information.

Conflict of interest statement. None declared.

REFERENCES

- Tang L, Nogales E and Ciferri C. Structure and function of SWI/SNF chromatin remodeling complexes and mechanistic implications for transcription. *Prog Biophys Mol Biol* 2010; **102**: 122–8.
- Wu JI, Lessard J and Crabtree GR. Understanding the words of chromatin regulation. *Cell* 2009; **136**: 200–6.
- Masliah-Planchon J, Bieche I and Guinebretiere JM *et al.* SWI/SNF chromatin remodeling and human malignancies. *Annu Rev Pathol* 2015; **10**: 145–71.
- Romero OA and Sanchez-Cespedes M. The SWI/SNF genetic blockade: effects in cell differentiation, cancer and developmental diseases. *Oncogene* 2014; **33**: 2681–9.
- Yamamoto S, Tsuda H and Takano M *et al.* Loss of ARID1A protein expression occurs as an early event in ovarian clear-cell carcinoma development and frequently coexists with PIK3CA mutations. *Mod Pathol* 2012; **25**: 615–24.
- Varela I, Tarpey P and Raine K *et al.* Exome sequencing identifies frequent mutation of the SWI/SNF complex gene PBRM1 in renal carcinoma. *Nature* 2011; **469**: 539–42.
- Li M, Zhao H and Zhang X *et al.* Inactivating mutations of the chromatin remodeling gene ARID2 in hepatocellular carcinoma. *Nat Genet* 2011; **43**: 828–9.
- Hodis E, Watson IR and Kryukov GV *et al.* A landscape of driver mutations in melanoma. *Cell* 2012; **150**: 251–63.
- Huang HT, Chen SM and Pan LB *et al.* Loss of function of SWI/SNF chromatin remodeling genes leads to genome instability of human lung cancer. *Oncol Rep* 2015; **33**: 283–91.
- Vicent GP, Zaurin R and Nacht AS *et al.* Two chromatin remodeling activities cooperate during activation of hormone responsive promoters. *PLoS Genet* 2009; **5**: e1000567.
- Xu F, Flowers S and Moran E. Essential role of ARID2 protein-containing SWI/SNF complex in tissue-specific gene expression. *J Biol Chem* 2012; **287**: 5033–41.
- Yan Z, Cui K and Murray DM *et al.* PBAF chromatin-remodeling complex requires a novel specificity subunit, BAF200, to regulate expression of selective interferon-responsive genes. *Genes Dev* 2005; **19**: 1662–7.
- Zhao H, Wang J and Han Y *et al.* ARID2: a new tumor suppressor gene in hepatocellular carcinoma. *Oncotarget* 2011; **2**: 886–91.
- Siegel RL, Miller KD and Jemal A. Cancer statistics, 2020. *CA Cancer J Clin* 2020; **70**: 7–30.
- Manceau G, Letouze E and Guichard C *et al.* Recurrent inactivating mutations of ARID2 in non-small cell lung carcinoma. *Int J Cancer* 2013; **132**: 2217–21.
- Jackson EL, Willis N and Mercer K *et al.* Analysis of lung tumor initiation and progression using conditional expression of oncogenic K-ras. *Genes Dev* 2001; **15**: 3243–8.
- Ji H, Ramsey MR and Hayes DN *et al.* LKB1 modulates lung cancer differentiation and metastasis. *Nature* 2007; **448**: 807–10.
- Gyorffy B, Surowiak P and Budczies J *et al.* Online survival analysis software to assess the prognostic value of biomarkers using transcriptomic data in non-small-cell lung cancer. *PLoS One* 2013; **8**: e82241.
- Li F, Han X and Wang R *et al.* LKB1 inactivation elicits a redox imbalance to modulate non-small cell lung cancer plasticity and therapeutic response. *Cancer Cell* 2015; **27**: 698–711.
- Duan Y, Tian L and Gao Q *et al.* Chromatin remodeling gene ARID2 targets cyclin D1 and cyclin E1 to suppress hepatoma cell progression. *Oncotarget* 2016; **7**: 45863–75.
- Raab JR, Resnick S and Magnuson T. Genome-wide transcriptional regulation mediated by biochemically distinct SWI/SNF complexes. *PLoS Genet* 2015; **11**: e1005748.
- Kakaroukas A, Ismail A and Chambers AL *et al.* Requirement for PBAF in transcriptional repression and repair at DNA breaks in actively transcribed regions of chromatin. *Mol Cell* 2014; **55**: 723–32.
- Boudesco C, Cause S and Jego G *et al.* Hsp70: a cancer target inside and outside the cell. *Methods Mol Biol* 2018; **1709**: 371–96.
- Rérole AL, Jego G and Garrido C. Hsp70: anti-apoptotic and tumorigenic protein. *Methods Mol Biol* 2011; **787**: 205–30.
- Koishi M, Yokota S and Mae T *et al.* The effects of KNK437, a novel inhibitor of heat shock protein synthesis, on the acquisition of thermotolerance in a murine transplantable tumor *in vivo*. *Clin Cancer Res* 2001; **7**: 215–9.

26. Ko SK, Kim J and Na DC *et al.* A small molecule inhibitor of ATPase activity of HSP70 induces apoptosis and has antitumor activities. *Chem Biol* 2015; **22**: 391–403.
27. Aso T, Uozaki H and Morita S *et al.* Loss of ARID1A, ARID1B, and ARID2 expression during progression of gastric cancer. *Anticancer Res* 2015; **35**: 6819–27.
28. Kovac M, Navas C and Horswell S *et al.* Recurrent chromosomal gains and heterogeneous driver mutations characterise papillary renal cancer evolution. *Nat Commun* 2015; **6**: 6336.
29. Daugaard M, Rohde M and Jaattela M. The heat shock protein 70 family: highly homologous proteins with overlapping and distinct functions. *FEBS Lett* 2007; **581**: 3702–10.
30. Wu CW, Biggar KK and Zhang J *et al.* Induction of antioxidant and heat shock protein responses during torpor in the gray mouse lemur, *microcebus murinus*. *Genom Proteom Bioinfo* 2015; **13**: 119–26.
31. Chuma M, Sakamoto M and Yamazaki K *et al.* Expression profiling in multistage hepatocarcinogenesis: identification of HSP70 as a molecular marker of early hepatocellular carcinoma. *Hepatology* 2003; **37**: 198–207.
32. Abe M, Manola JB and Oh WK *et al.* Plasma levels of heat shock protein 70 in patients with prostate cancer: a potential biomarker for prostate cancer. *Clin Prostate Cancer* 2004; **3**: 49–53.
33. Hwang TS, Han HS and Choi HK *et al.* Differential, stage-dependent expression of Hsp70, Hsp110 and Bcl-2 in colorectal cancer. *J Gastroenterol Hepatol* 2003; **18**: 690–700.
34. Malusecka E, Zborek A and Krzyzowska-Gruca S *et al.* Expression of heat shock proteins HSP70 and HSP27 in primary non-small cell lung carcinomas. An immunohistochemical study. *Anticancer Res* 2001; **21**: 1015–21.
35. Assimon VA, Gillies AT and Rauch JN *et al.* Hsp70 protein complexes as drug targets. *Curr Pharm Des* 2013; **19**: 404–17.
36. Moradi-Marjaneh R, Paseban M and Moradi Marjaneh M. Hsp70 inhibitors: implications for the treatment of colorectal cancer. *IUBMB Life* 2019; **71**: 1834–45.
37. Yaglom JA, Wang Y and Li A *et al.* Cancer cell responses to Hsp70 inhibitor JG-98: comparison with Hsp90 inhibitors and finding synergistic drug combinations. *Sci Rep* 2018; **8**: 3010.
38. Kumar S, Stokes J, 3rd and Singh UP *et al.* Targeting Hsp70: a possible therapy for cancer. *Cancer Lett* 2016; **374**: 156–66.
39. He L, Tian X and Zhang H *et al.* BAF200 is required for heart morphogenesis and coronary artery development. *PLoS One* 2014; **9**: e109493.